
Accretion onto strongly magnetized neutron stars

Master project

Supervisor: PD Dr. A. A. Hujeirat

David Gobrecht

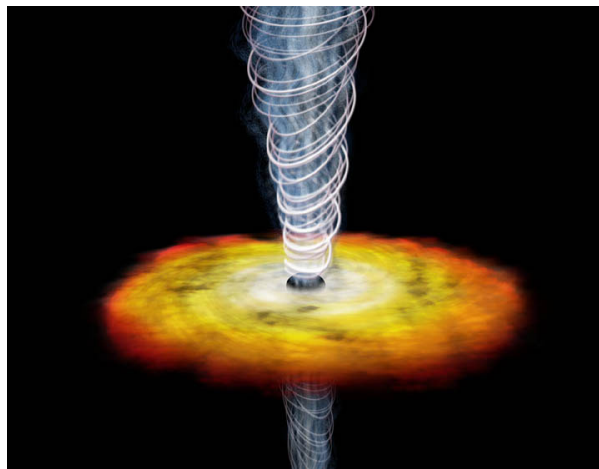
January 16, 2010

Abstract

In this project the fundamentals of accretion phenomena onto ultra-compact neutron stars (NS) and their connection to the formation and acceleration of ultra-relativistic jets are presented and discussed. From basic physics we know that gravitationally-bound rotating plasmas around compact objects form accretion disks. Depending on their Mass-to-kinetic energy ratio, they may become geometrically thin or thick. As all normal stars in the local universe are observed to rotate sub-Keplerian, a boundary layer between the accretion disk and the slowly rotating central object must form, where the rotational velocity of the inflowing matter deviates significantly from the corresponding Keplerian profile. In the case of a strongly magnetized NS, the disk truncates at a certain radius, where the inflowing matter start collimating along the magnetic field lines and shocks as it hits the solid surface in the polar cap, thereby emitting hard x-rays. Accretion disks around weakly magnetized NS's however are expected to penetrate deeper in the gravitational well of the NS, giving rise to plasma ejection from the boundary layer that subsequently collimate into jets. Magnetic fields both of the NS and of the accreted disk-matter are considered to be efficient converters of rotational into kinetic and magnetic energies that power most of the jets observed in X-ray binaries and in active galactic nuclei. Depending on ratio of mass-to-total energy of the jet, the jet content can either be leptonic or hadronic-dominated, though the latter is preferable.

Contents

1	Introduction	3
2	Accretion disks	3
2.1	Viscosity	3
2.2	Standard disk	5
2.3	Steady-state accretion	6
2.4	Thermodynamics and radiation	6
2.5	Instabilities	8
3	Accretion on neutron stars	9
3.1	Truncated disk	9
3.2	Magnetized neutron star	11
3.3	Accretion column structure	15
3.4	Accretion induced pulses in columns	22
4	Accretion powered Jets	23
4.1	Disk-Jet coupling	23
4.2	A model of disk-jet connection for AGN's	24
4.3	Jet	25
5	Conclusion	26



1 Introduction

Accretion disks and stellar binaries have been of enormous astronomical interest since they were discovered. They are responsible for phenomena such as jet formation, X-ray bursts etc. For the latter see Hujeriat & Thielemann (2009). Accretion is a process, where a cosmic object accumulates surrounding matter due to gravitational attraction. Such an object could be a protostar, white dwarf (WD), neutron star (NS) or a black hole (BH). This accretion process acts like a flow, wherein particles interact in pairs. Therefore accretion is at first described by fluid dynamics. A further, more precise description is necessary, if magnetic fields play a role (MHD). If the accreting object is compact, as it is the case for NS, another modification of the presented model should be included: General relativity (GR).

The accretion of matter includes also the release of gravitational energy via kinetic (thermal) and electromagnetic energies. A set of radiative processes is aligned to accretion including Bremsstrahlung, synchrotron -, Compton -, and thermal black body radiation. Accretion systems are very efficient 'machineries' exploiting 10 to 15 percent of the available accretion energy which is quite impressive in comparison to hydrogen burning of the sun having an efficiency of 0.7 percent. As anticipated accretion physics covers a diversity of disciplines such as Newtonian and relativistic gravitation, electrodynamics including magnetic and radiative processes, hydrodynamics and thermodynamics.

As far as today cataclysmic variables are well-studied and understood since their variability in some cases takes place on timescales less than a day and are therefore good candidates for observations. Compact objects like black holes or neutron stars generally behave different; here the accretion flow is rather constant and not stimulated periodically like in (dwarf) novae, what can be directly seen by luminosity observations. Another point is that NS and BH are relativistic objects and they cannot be described in a good approximation by special relativity as white dwarf do. Due to sufficient strong magnetic fields which are in super equipartition with thermal energy in NS/BH's the standard inflow of Keplerian motion will be disrupted and a truncated disk results. This truncated part is referred to the boundary layer (BL) in which relativistic jets form and in which magnetic reconnection occurs. Therefore it is necessary to deal with 3D axis-symmetric MHD including general relativity. This only can be realized by numerical simulations which I will intend to do in future works. In section 2 the general case of disk accretion will be discussed, then the magnetized disk case will be included (section 3). In section 4 the outflow (jet) and its connection to disk accretion are described and an example model is presented. Finally concluding statements will be made in section 5.

2 Accretion disks

2.1 Viscosity

Viscosity is a microscopic property of fluids and describes the inner friction of the fluid, i.e. the movability of constituent particles. Despite of this fact viscosity has

influence on the behaviour of the whole disk. Viscosity can have several origins, in the case of an accretion disk it is due to the shear effect of its preassumed Keplerian rotation.

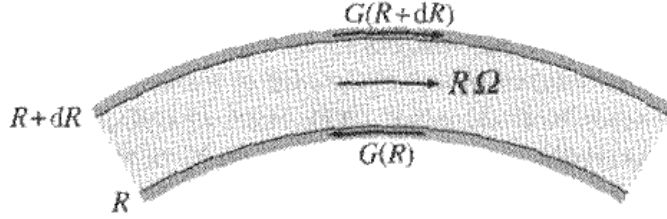


Figure 1: Shear effect of differential Keplerian rotation: $\frac{\partial\Omega}{\partial R} \neq 0$

This effect enters the conservation of angular momentum as an additional viscous torque G which is given by

$$G(R) = 2\pi R\nu\Sigma R^2 \frac{\partial\Omega}{\partial R}, \quad (1)$$

where Σ denotes the surface density, ν the viscosity, R the distance from the centre and Ω the angular velocity.

In the following figure it is obvious that with increasing time expressed by the dimensionless variable $\tau = 12\nu t R_0^{-2}$ the original annulus at radius R_0 becomes a geometrically thin disk i.e. the surface density Σ is distributed in a large range of radii after a sufficient long time $t_{visc} \sim \frac{R}{v_R}$, where v_R is the radial or drift velocity. This is possible since accreting gas must lose angular momentum. Because total angular momentum must be conserved, other (non-accreting) gas particles must gain angular momentum and move outward.

This yields on one hand the radial or viscous timescale t_{visc} and on the other hand the important assumption of a thin disk on viscous timescales. Tightening this assumption consider a high accretion rate $0.01 - 1M_{edd}$ (Pringle 1981), then the gas density is high, so the gas is able to radiate efficiently and stay geometrically thin. However, if the gas density is low, the gas may be unable to radiate energy at a rate that balances viscous heating (see Section 2.5). In this case, the heat generated by viscosity will be advected inwards with the flow instead of being radiated. The disk becomes hot, hence geometrically thick (quasi-spherical) and optically thin (hence low density). Such accretion scenarios are called 'Advection Dominated Accretion Flows' (ADAF's). For ADAF solutions see My report describes mainly geometrically thin disk regimes. So viscous stresses caused by the shearing effect of differential rotation are responsible for the transport of angular momentum. These stresses also heats the disk gas. Detailed studies suggest that hydrodynamic mechanisms, namely the above described viscosity, alone will not produce sustained turbulence in differentially rotating disks to transport angular momentum (see, e.g., Hawley et al. 1998). So another effect has to be included: MHD (magneto-rotational) instabilities in a differentially rotating, magnetized disk drive turbulence (consuming the rotational energy), which in turn has the effect of viscosity. Magnetic effects will be

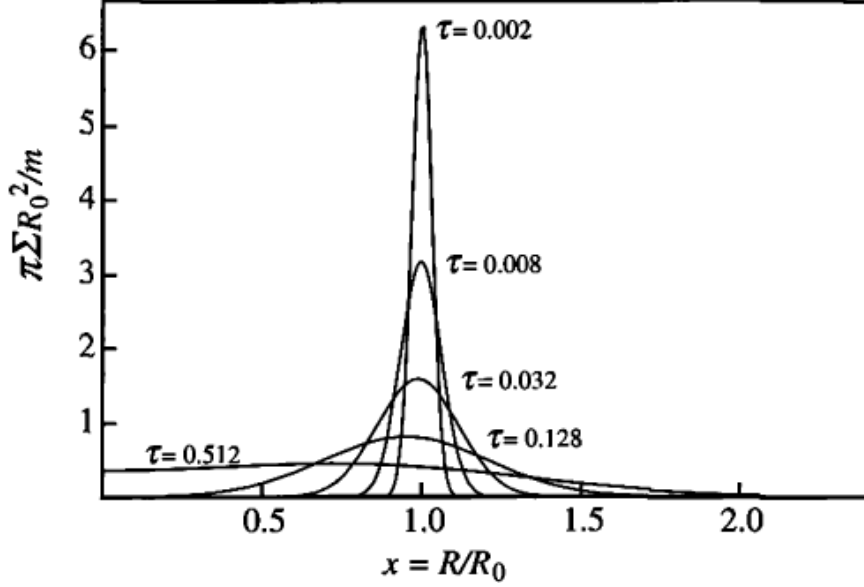


Figure 2: Graph of the mass distribution for different times. After sufficient time the original annulus at $R = R_0$ has extended to a spreaded disk

considered in the next section. It is still not yet considered the magnitude and the behavior of the viscosity ν . This will be done in the next subsection.

2.2 Standard disk

As known from classical fluid dynamics molecular viscosity is given by $\nu \simeq v_{th}\lambda_{mfp}$ which has the dimensions of cm^2s^{-1} . In case of accretion disks one deals with turbulent viscosity. An α -disk, or standard disk, is an accreting system which includes an accretor, (e.g. white dwarfs, neutron stars, black holes). The prescription α originates from Shakura and Sunyaev who describe viscosity with a parameter α between its maximum (= local sound speed c_s) and its minimum value (= 0). So we can impose the turbulent viscosity as:

$$\nu = \alpha c_s H_d \text{ with } \alpha \in [0, 1], \quad (2)$$

where H_d denotes the half-thickness of the disk.

This parametrisation is due to the complexity and uncertainty of turbulent viscosity processes. This allows qualitative statements and estimations of magnitudes of relevant quantities such as density ρ , height of the disk H_d , energy equation and pressure. Typical models of disks recently performed have $\alpha = 0.01 - 0.1$. (see e.g. Hujeriat & Thielemann (2009)). It is not yet clear how the α -prescription matches to a real accretion disk, which, at present, only can be described and simulated numerically.

2.3 Steady-state accretion

Considering the 3D MHD differential equations, important simplifications occur if a steady state ($\frac{\partial}{\partial t} = 0$) is required. In particular, when integrating the continuity equation a constant accretion rate \dot{M} at every radius results

$$\dot{M} = -2\pi R\Sigma v_R = \text{const.} \quad \forall R, \quad (3)$$

where v_R is the radial velocity. Another consequence is that in the case of a Keplerian disk the angular momentum equation can be manipulated to yield (see, e.g. Frank et. al 1992)

$$\nu\Sigma = \frac{\dot{M}}{3\pi} \left(1 - \left(\frac{R}{R_*}\right)^{\frac{1}{2}}\right), \quad (4)$$

where R_* is the radius of the accretor.

2.4 Thermodynamics and radiation

An accreting compact object like a neutron star serves as a very powerful engine. It converts the matter inflow at least partially into radiation. Insights how this 'machinery' works are given by thermodynamical relations including viscous processes, namely the heating function or, more precisely, dissipation rate per unit area $D(R)$ given by.

$$D(R) = \frac{3GM\dot{M}}{8\pi R^3} \left(1 - \left(\frac{R_*}{R}\right)^{\frac{1}{2}}\right) = \frac{1}{2}\nu\Sigma \left(R\frac{\partial\Omega}{\partial R}\right)^2, \quad (5)$$

where G is the gravitational constant and M the mass of the accretor.

Surprisingly the viscosity ν vanishes in the dissipation rate, a consequence of mass, energy and angular momentum conservation and of the implicit assumption of self-adjusting viscosity on according timescales. $D(R)$ is necessary to obtain the luminosity, a observable quantity and therefore a very important one since it gives constraints to the different models:

$$L = 2 \int_{R_*}^{\infty} 2\pi R D(R) dR = \frac{GM\dot{M}}{2R_*} = \frac{1}{2}L_{acc}, \quad (6)$$

that means that half of the total available luminosity, which consist of accretion-liberated gravitational energy, can be radiated away from the BL whereas the other part is lost by the plasma while spiraling in, i.e. goes into rotational energy, which may be either dissipated in a BL or, in the case of a BH, swallowed. Assigned to energy this fact satisfies the virial theorem $E_{kin} = 0.5E_{pot}$.

The thin disk approximation implies that pressure and temperature gradient are essentially vertical. The pressure P then is given by gas and radiation pressure:

$$P = \frac{\rho}{\mu m_H} K T_c + \frac{4\sigma}{3c} T_c^4, \quad (7)$$

where ρ is the density, μ the reduced mass, m_H the atomic mass, σ the Stefan-Boltzmann constant, c the light velocity, K the Boltzmann constant and T_c the central temperature. Temperature is usually related to an energy equation. Since it change mainly in z-direction radiative or convective energy transport is possible. Taking the first as the most propable the radiation flux F reads

$$F(z) = -\frac{16\sigma T^3}{3\kappa_R \rho} \frac{\partial T}{\partial z}, \quad (8)$$

where κ_R is the Rosseland mean opacity and z goes in vertical direction. For obtaining the total dissipation rate per unit volume $D(R)$ the difference of flux from centre to disk height has to be calculated

$$D(R) = F(H) - F(O) = \int_0^H Q^+ dz, \quad (9)$$

where Q^+ is the volume rate of heating by dissipation. The model presented here implies an optically thick and geometrically thin accretion disk. The first fact can be express by the optical depth

$$\tau = \rho \kappa_R H \gg 1, \quad (10)$$

where H is the vertical height. The Rosseland mean opacity, the dominant opacity for neutron stars, since in sufficient hot and compact stars electron scattering (Thompson scattering) is the dominant process. The assumption above simplifies the problem since optically thick regimes are described as blackbody radiators; else radiation can escape directly which lead to fast cooling. Hence we can write the flux as

$$F(z) \sim \frac{4\sigma}{3\tau} T_c^4. \quad (11)$$

Since the temperature steepens quickly in z-direction: $T_c^4 \gg T(H \neq 0)$ and therefore

$$D(R) = \frac{4\sigma}{3\tau} T_c^4. \quad (12)$$

This is the required energy equation, which also gives a connection to the radial temperature distribution, since the disk radiates as BB

$$T(R) = \left(\frac{D(R)}{\sigma} \right)^{\frac{1}{4}} = \left(\frac{3GM\dot{M}}{8\pi\sigma R^3} \left[1 - \left(\frac{R_*}{R} \right)^{\frac{1}{2}} \right] \right)^{\frac{1}{4}}, \quad (13)$$

which has a maximum of $0.488T_*$ at a distance of $\frac{49}{36}R_*$ which is well outside the star, i.e. in the disk.

Since the disk radiates its spectra almost as blackbody, the blackbody spectral intensity I_ν is given by

$$I_\nu = \frac{2h\nu^3}{c^2 [\exp(\frac{h\nu}{KT(R)}) - 1]}, \quad (14)$$

where h is the Planck constant and ν the frequency of the photon. For an observer at a distance D and inclination i , i.e. an angle i of the normal of the disk to the line of sight the spectral flux is given by

$$F_\nu = \frac{2\pi \cos(i)}{D^2} \int_{R_*}^{R_{out}} I_\nu R dR = \frac{4\pi h \cos(i) \nu^3}{c^2 D^2} \int_{R_*}^{R_{out}} \frac{R dR}{\exp(\frac{h\nu}{KT(R)}) - 1}. \quad (15)$$

This result is independent of viscosity and comes from steady and blackbody assumption.

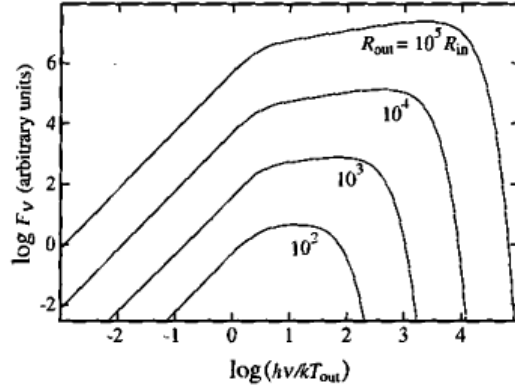


Figure 3: Spectra (radiative flux) in dependence of the photon energy for different outer radii R_{out} of a disk

The spectra is divisible in three regimes:

- Rayleigh-Jeans: $h\nu \ll KT(R_{out})$: $F_\nu \propto \nu^2$
- Intermediate case: $h\nu \simeq KT(R_{out})$: $F_\nu \propto \nu^{\frac{1}{3}}$
- Wien: $h\nu \gg KT(R_{out})$: $F_\nu \propto \exp(-\nu)$

The intermediate case, i.e. the so called continuum or flat spectrum ($\propto \nu^{\frac{1}{3}}$) corresponds to characteristic accretion disk spectra. But since the temperature varies appreciably with the radius $T(R_{out}) \ll T(R_*)$ various frequency contributions produce an overlap of different maximum frequencies with different intensities.

2.5 Instabilities

In a steady and thin disk no instabilities exist since it is stable against small perturbations. Therefore it is necessary to include timescales on which instabilities can grow. The viscous timescale was already encountered. But there exist further ones (ordered by increasing timescale): dynamical or rotational, vertical static and thermal. The latter is among the most important one concerning accretion disks. The thermal timescale is defined by the fraction of heat content per unit disc area to dissipation rate per unit disc area or

$$\tau_{th} = \frac{\text{heat - content/area}}{\text{dissipation - rate/area}} = \frac{PH}{D(R)} = \frac{\Sigma c_s^2}{\frac{3GM\dot{M}}{8\pi R^3(1-\frac{R_*}{R})^{1/2}}} = \frac{8R^3 c_s^2}{9GM\nu}. \quad (16)$$

This time is necessary for a readjustment of thermal changes. Since the thermal instability grows on much shorter times than the viscous one, but on longer timescales compared to dynamical and hydrostatical instability the assumptions made here are 1) the surface mass density Σ remains constant since only viscosity can change it significantly and 2) the vertical structure remains constant since thermal changes may be balanced by the faster dynamic response.

3 Accretion on neutron stars

3.1 Truncated disk

The α parametrisation works in accretion disks like white dwarf disks, but it fails if there exist a sufficient strong magnetic field of external or intrinsic origin near the surface of the accretor. This field is strong enough and builds the so called boundary layer (BL), where the local angular velocity of disk particles becomes sub-keplerian (see Figure 4) and therefore

$$\Omega_{BL} \leq \Omega_{Kep} = \sqrt{\frac{GM}{R^3}}, \quad (17)$$

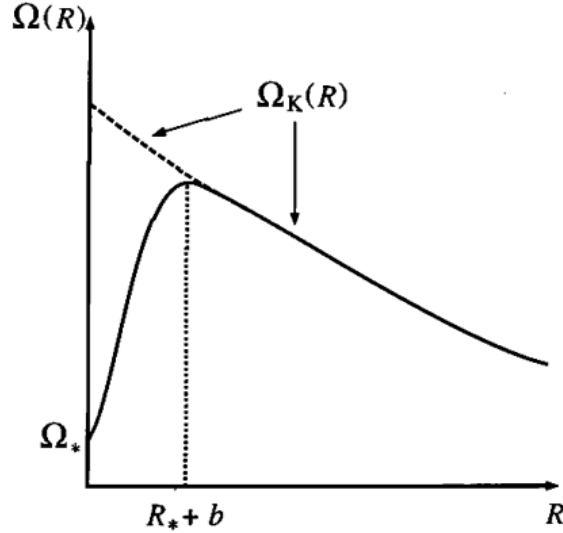


Figure 4: In the boundary layer (BL) is located next to the stellar surface between R_* and $R_* + b$. Here the angular motion is sub-Keplerian and the matter flows in

which means the boundary layer is located between the surface of the compact object R_* and his radial extend $R_* + b$. The nature of the unexpected

slower motion in the BL is due to the effect of the constancy of the magnetic flux $\phi = Br^2$, which implies $B \propto r^{-2}$. The rotation of the accretor and the disk respectively lead to freezing the field lines in the moving matter (flux freezing), so the field lines become twisted. But this cannot hold for long time and twisted lines can slip. The stressing of the lines due to differential rotation decelerates the part of the disk in the BL.

Consider the radial momentum equation

$$v_R \frac{\partial v_R}{\partial R} - \frac{v_\Phi^2}{R} + \frac{1}{\rho} \frac{\partial P}{\partial R} + \frac{GM}{R^2} = 0, \quad (18)$$

where the centrifugal term $\frac{v_\Phi^2}{R} = \Omega(R)^2 R$ is always smaller as the gravity term $\frac{GM}{R^2} = \Omega_{Kep}^2 R$ in the boundary layer (see Figure 4), the pressure term $\frac{1}{\rho} \frac{\partial P}{\partial R}$ and the radial term $v_R \frac{\partial v_R}{\partial R}$ must compensate this unbalance. Neglecting the differentials the radial term becomes $\frac{v_R^2}{b}$ and the pressure term $\frac{P}{\rho R} \sim \frac{c_s^2}{b}$ where we used the definition of the sound speed. By assumption ($c_s^2 > v_R^2$) the main balancing contribution arises in the pressure gradient term. Hence in the BL located next to the surface R_* the condition

$$\frac{c_s^2}{b} \sim \frac{GM}{R_*^2} \quad (19)$$

leads to the radial BL size of $b \sim \frac{R_*^2 c_s^2}{GM}$. For the vertical size of the hydrostatic equilibrium in z-direction is pulled up:

$$\frac{1}{\rho} \frac{\partial P}{\partial z} = \frac{\partial}{\partial z} \left(\frac{GM}{(R^2 + z^2)^{\frac{1}{2}}} \right) = -\frac{GMz}{R^3}, \quad (20)$$

where the thin disk approximation ($z \ll R$) was used in the last step. Again the differentials are neglected and the scale height H is set to be $\sim z$. So the height H inside the BL seems to be

$$H \sim c_s \sqrt{\frac{R_*^3}{GM}} \quad (21)$$

Collecting these results justifies our assumption of a geometrically thin BL, namely $b \ll R_*$ and gives an idea of the boundary layers geometrical dimensions as shown in Figure 4, where

$$b \sim \frac{H^2}{R_*} \ll H \ll R_*. \quad (22)$$

The BL emits radiation from a regime as shown in Figure 4 on two faces of the disk. If in this regime the accretion rate and implicitly the density is high enough, the BL is an optically thick region. So the BL is treated as black body radiator (BB) emitting through a surface of $S = 2 \cdot 2\pi R_* H$. Since half of the total available accretion luminosity is consumed by the disk itself and the other half is released in the BL, the luminosity equation becomes

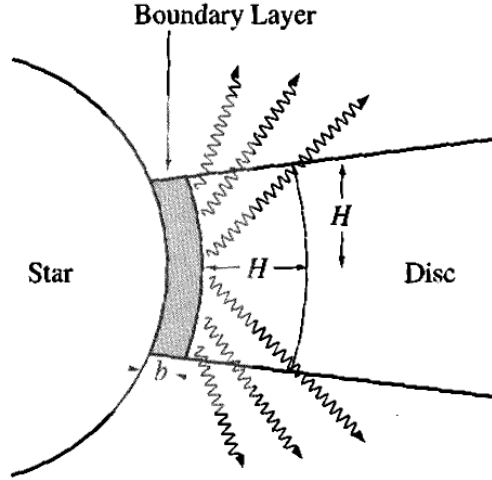


Figure 5: A schematic picture of the geometry of the boundary layer (BL) emitting X-rays and other radiation

$$S\sigma T_{BL}^4 \simeq \frac{GM\dot{M}}{2R_*}, \quad (23)$$

where T_{BL} denotes the temperature of the BL. Comparing this with the accretor temperature yields

$$T_{BL} \sim \left(\frac{R_*}{H}\right)^{\frac{1}{4}} T_*. \quad (24)$$

Define a shock temperature T_s at which the bulk velocity of the gas transits the sonic point (i.e. near the surface the accreting gas will have velocities close to that of free-fall and therefore highly supersonic)

$$T_s = \frac{3GMT_*}{8c_s^2 R_*}. \quad (25)$$

As clearly can be seen is that the temperature of the boundary layer exceeds the one of the star, but not by a large factor. This phenomena exists also in the solar case, where the corona is hotter than the surface of the sun. Since the maximum temperature in the disk is less than half of the surface temperature, the hottest part of the system is really the BL. As the BL is considered as black body the internal structure discussion is evitable for the moment. However viscosity effects, which are due to the strong shearing ($\propto \frac{\partial\Omega}{\partial R}$) in the BL quite keen, are disregarded in the BB assumption. This effect is even stronger, if we consider an optical thin disk (ADAF solutions)

3.2 Magnetized neutron star

Neutron stars often possess an intrinsic strong magnetic field of the order of $10^{12}G$. Due to their enormous density $\rho_c = 10^{14} - 2.5 \cdot 10^{15} \frac{g}{cm^3}$ and their mass

$M_{NS} \sim 1.4M_{\odot}$ their radii are in the order of $R \sim 10km$. NS's are not burning fuel and rest of their internal (thermal) and rotational energy. The strong magnetic field disrupts the disc flow at a certain radius R_M , where the thermal and the magnetic energy are in equipartition, i.e. $nKT \sim \frac{B^2}{8\pi}$. Inside this radius the dipole-like magnetic field is of large scale and so supresses turbulence or other thermal motions of the plasma in the disk. The dipole field becomes weak and does not control the inflow outside R_M . In this regime field lines reconnect on small scales, thus a large-scaled polodial-straightened field cannot be maintained. At R_M the PMF disrupts the standard disk flow in a complex way. A schematic picture is shown in the following

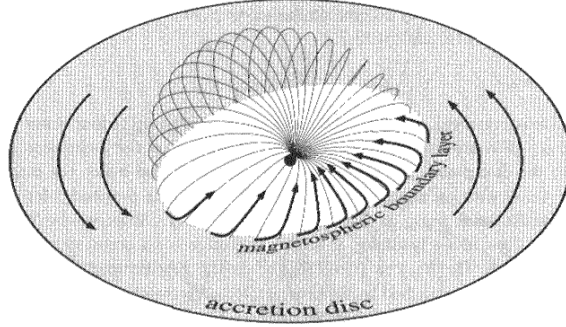


Figure 6: Disruption of the accretion flow due to the magnetospheric boundary layer

For dipole magnetic fields the radial dependance is given by the Biot-Savart law

$$dB \propto \frac{Idl}{R^3}, \quad (26)$$

where I is the current and dl is an infinitesimal length of a conductor. From this law one can demand the constancy of the magnetic momentum

$$\mu_{mag} \simeq B_* R_*^3 \simeq B(R) R^3 \simeq const. \quad (27)$$

Introducing the magnetic pressure P_{mag} , the energy density which is associated with the magnetic field and which is identical to any other physical pressure except that it is carried by the magnetic field rather than kinetic energy of the gas particles. Based on the Biot-Savart-law (26) the pressure increases rapidly when moving towards the stellar surface

$$P_{mag} = \frac{B^2}{8\pi} = \frac{B_*^2 R_*^6}{8\pi R^6}. \quad (28)$$

The spherical symmetrical accretion flow is being disturbed by p_{mag} (see figure). As a consequence it exceeds ram and gas pressures at some radius R_M . In a supersonic regime the ram pressure $P_{ram} = \rho v^2$ contributes dominantly, since the gas reaches almost free fall velocities $v_{ff} = \sqrt{\frac{2GM}{R}}$. Hence the demanded equilibrium at R_M is

$$P_{mag}(R_M) = P_{ram}\Big|_{R_M}. \quad (29)$$

Evaluating this equation by imposing the steady state assumption, namely a constant accretion rate of $\dot{M} = 4\pi R^2 \rho(-v)$ gives

$$P_{ram}\Big|_{R_M} = |\rho v| v_{ff} = \frac{\sqrt{2GM\dot{M}}}{4\pi R_M^{5/2}}, \quad (30)$$

which terminates the so called Alfvén radius

$$R_M = (8G)^{-\frac{1}{7}} \mu_{mag}^{\frac{4}{7}} M^{-\frac{1}{7}} \dot{M}^{-\frac{2}{7}}. \quad (31)$$

Since the accretion rate is not directly observable, often the Eddington luminosity $L_{edd} = \frac{4\pi MGm_H c}{\sigma_T}$, especially for X-ray sources, is used to calculate this radius R_M numerically (Frank et al. 1992) as

$$R_M = 2.9 \cdot 10^8 M^{-\frac{1}{7}} R_6^{-\frac{2}{7}} L_{37}^{-\frac{2}{7}} \mu_{30}^{\frac{4}{7}} \simeq 3 \cdot 10^8 cm. \quad (32)$$

where M is the mass in solar units, R_6 the radius in $10^6 cm$, L_{37} the luminosity in $10^{37} erg/s$ and μ_{30} the magnetic moment in $10^{30} Gcm^3$.

This result is of crude parametrised nature, but believable in order of magnitude, since P_{mag} decreases rapidly with R . A source of error consists in the fact that magnetic fields can cause plenty of instabilities (e.g. Balbus-Hawley instability). At the moment it is assumed that inside R_M the plasma flow travels along the magnetic field lines. So at this point the torque exerted by the magnetic field should be in order of the viscous torque (see Equation (1)) The latter can be described as transport rate of specific angular momentum $\dot{M}L_{spec} = \dot{M}R_M^2\Omega(R_M)$ assuming steady state regime. More complicated is it to describe the magnetic torque involving the toroidal component B_ϕ of the disturbed dipole field. These distortions are effected by the magneto(-rotational) instabilities mentioned above. Several estimations have led to the similar answer

$$r_M \sim 0.5R_M, \quad (33)$$

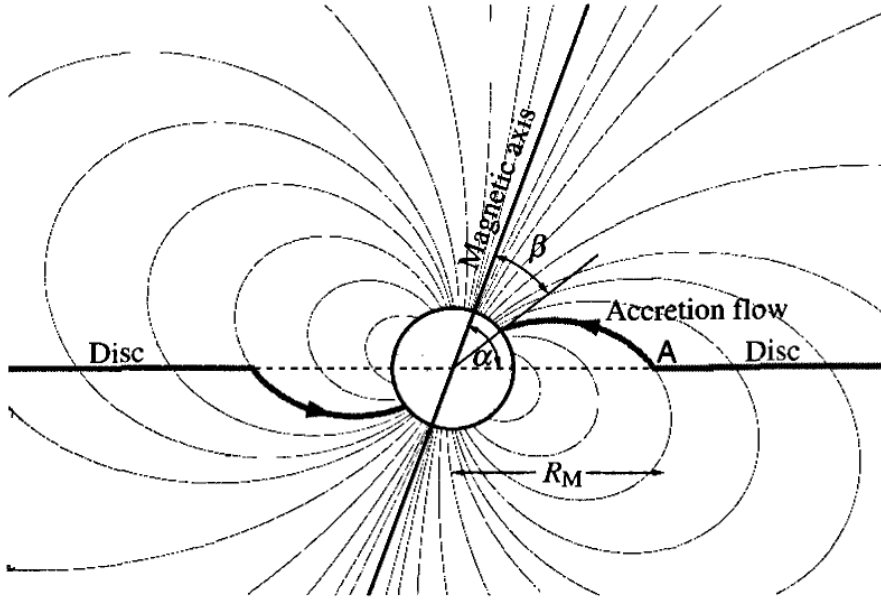
where r_M is the radius where viscous and magnetic torque are believed to be in the same order. Of course r_M is dependant of the angle α between dipole axis and disk plane. r_M is well outside the neutron star radius $R_* \cong 10^6 cm$ in most cases and therefore accretion is controlled by the magnetic field near the surface. This is due to the fact that the luminosity cannot exceed the Eddington luminosity, else the accretion would be halted, i.e. L_{37} cannot be greater than 13, and M and R_6 are in order of unity. A surface magnetic field of less than $10^9 G$ would result for $r_M < R_*$ which is a quite faint field for neutron stars. On the other hand r_M is not too great to (completely) hinder or even terminate the formation of a disk as a whole since the circularization radius R_{circ} , a lower limit for any accretion disk, is always greater than r_M .

Consider the general case of a rotating accretor with a corotating magnetic field with angular velocity Ω_* and a to Ω_* perpendicular accretion disk with same sense of rotation. In our steady-inflow regime the angular velocity Ω_*

must be sub-keplerian or, more precisely, smaller than the angular velocity at r_M . To express this fact the fastness parameter is defined by

$$\omega_* = \frac{\Omega_*}{\Omega_K(r_M)} < 1. \quad (34)$$

Otherwise particles would drift along the field lines towards larger radii due to the centrifugal repulsion. Fortunately, magnetic controlled accretion differs from the unmagnetized case observationally: The inflow touches only a small fraction of the neutron star surface. To trace the accretion flow consider the following picture



At A particles leave the disk and spirals along the magnetic field lines towards the polecaps of the accretor. In this two dimensional consideration polar coordinates (R, ϕ) are used and therefore the dipole geometry of the field lines is $R = C \sin^2(\phi)$ where C denotes a line specific constant. At A is $R = r_M$ and $\phi = \alpha$ respectively; this implies $C = r_M \sin^{-2}(\alpha)$. The minimal angle between disk and the field line crossing the surface is β which implies the following condition

$$\sin^2(\beta) = \frac{R_*}{r_M} \sin^2(\alpha) \quad (35)$$

Under neglect of thermal or magnetic instabilities it is possible to impose a limit for the angle β , since for higher colatitudes the corresponding field line cross the disk in a region where $R < r_M$. Thus accretion takes place on an area around pole capes limited by β . The fraction of this area to the surface is then

$$f_{disk} = \frac{\pi R_*^2 \sin^2(\beta)}{4\pi R_*^2} = \frac{R_* \sin^2(\alpha)}{4r_M} \quad (36)$$

which has to be multiplied by factor 2, since in a dipole field exist per definition two poles and it is in order of $0.1 - 0.0001$ depending on $r_M = r_M(L, \mu)$. L and μ are limited by the Eddington luminosity as already mentioned in this section. An important effect is that a part of accretion luminosity is periodically modulated (observationally) which is a definitive hint for rotating luminescent accreting systems. This pulsation effect becomes stronger as more collimated the accreting polecap is. The frequency of pulsation decrease with time due to extraction of rotational energy. Remind the fastness parameter defined above, it can be distinguished between slow rotators with $\omega_* \ll 1$ and faster rotators. In the latter case effects like wind carrying away angular momentum or interaction of the magnetic field beyond r_M could happen. In the slow case accretion of angular momentum at r_M occurs due to the torque effect. Considering the change of spin due to this effect while supposing the disk and the star have the same sense of rotation leads to

$$I\omega_* = \dot{M}r_M^2\Omega_K(r_M) = \dot{M}\sqrt{GMr_M} = \frac{RL_{acc}}{GM}\sqrt{GMr_M}, \quad (37)$$

where I is the moment of inertia. With the rough value of r_M it is possible to calculate the change of periodicity, frequency ν respectively

$$\dot{\nu} = 2.7 \cdot 10^{-12} M^{-\frac{3}{7}} R_6^{\frac{6}{7}} L_{37}^{\frac{6}{7}} \mu_{30}^{\frac{2}{7}} I_{45}^{-1} \frac{Hz}{s}, \quad (38)$$

where M is the mass in solar units and I_{45} the moment of inertia in $10^{45} gcm^2$. For a given accretion rate, it is easily for NS's with the angular velocity of the accretor ω_* . Under certain conditions the spin-up rate can be 10^5 times faster than in the white dwarf case. This difference is due to the small moment of inertia I of NS's.

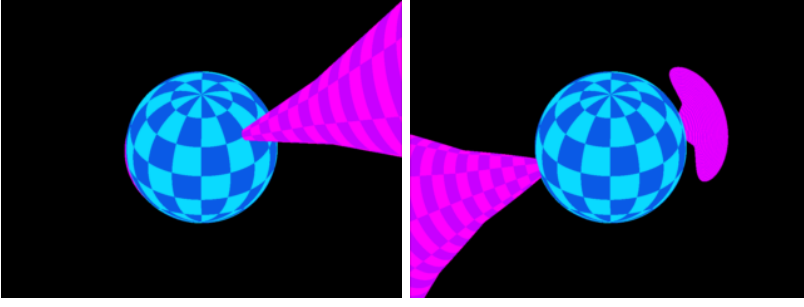
Slow rotators also can be described by the corotation radius. At this radius particles attached to a fieldline rotate Keplerian. Therefore R_Ω should be greater than r_M to have magnetic controlled inflow. The corotation radius is given by

$$R_\Omega = \left(\frac{GMP_{spin}^2}{4\pi^2} \right)^{\frac{1}{3}} = 1.5 \cdot 10^8 P_{spin}^{\frac{2}{3}} M^{\frac{1}{3}} cm. \quad (39)$$

3.3 Accretion column structure

The accretion column is based on a column which is of this geometric form due to the limited inflow area at the surface of a neutron star. To give an impression, consider the following pictures with two different columns.

These appear also in magnetized white dwarf accretion systems, but in the NS case extreme conditions such as free fall velocities of $0.5c$, magnetic fields of $10^{12}G$ and Eddington luminosity can be reached. The question that may arise is, if there occur shocks in these matter-filled, cylindrical columns. Inside R_M the column the inflow is magnetically controlled, as the magnetic pressure is larger than the dynamical pressure of freely falling matter. At a low accretion rate the accreting plasma falls freely onto the stellar surface and decelerated by particle



interaction in the neutron star photosphere (Basko and Sunyaev, 1976). But it is still uncertain, if shocks really occur, even if the flow is perfectly homogenous. To prove this, consider the mean free path concerning deflection

$$\lambda_d = v\tau_d = \frac{m^2 v^4}{2\pi n e^2 \ln \Lambda}, \quad (40)$$

where τ_d is the deflection time, m the mass, v the velocity, n the number density, e the elementary charge and Λ is the fraction of the maximal to the minimal impact parameter.

To get an estimation of the order of magnitude, the continuity equation is used and modified by the fact that f_{disk} limits the surface of matter flow; velocities of $v \sim 0.5c$, $m = m_p$ and $\ln \Lambda = 20$ are assumed. This implies a density of

$$n = 10^{16} \dot{M}_{16} f_{disk}^{-1} cm^{-3}, \quad (41)$$

where \dot{M}_{16} is the accretion rate in $10^{16} g/s$. This is very large in comparison to the length scale of the neutron star (which is typically the radius of $R_* \sim 10^6 cm$), since $\dot{M}_{16} f^{-1} < 100$ is limited by the Eddington luminosity and the fraction of the surface, where matter flows in. Thus a collisional ion (proton) shock here is impossible; but it does not exclude any kind of shock i.e. where fluid properties change significantly (discontinuously). So one has to include *collisionless* shocks. The reason such a structure can exist is because particles interact with each other not through Coulomb collisions, but by the emission and absorption of collective excitations of the plasma called plasma waves (Laming 2009), which is not well-understood. Because of the nescience of collisionless shocks and their conditions, both cases (existence and non-existence) have to be regarded. Additionally the strong magnetic field including many microscopic processes taking place simultaneously complicates this fact for the neutron star case. Thus, a process different from viscosity has to be responsible for the dissipation of the ordered energy; means a process operating on smaller scales $\sim \lambda_d$ than viscosity. A further complication comes from observations implying luminosities close to the Eddington limit: this is in conflict with the limitation of modest, but not faint ($\eta \sim 0.1 - 0.15$) accretion rates. These uncertainties could be amplified by complex geometries of the radiative transfer, hence a ad hoc simple radiation transfer described above is rather improbable.

Before treating some column models theory about plasma motion, particularly

about deceleration, should be investigated. Suppose an suprathemal incident test particle(here: an electron with velocity U) on a plasma (here: consists of protons), which is itself in thermal equilibrium and thus

$$\frac{1}{2}m_e U^2 \gg \frac{1}{2}m_p v_{th}^2 = \frac{3}{2}KT. \quad (42)$$

Defining a slowing down timescale t_s for the incident, non-relativistic particle (after Boyd and Sanderson 1969)

$$t_s = -\frac{U}{dU/dt} = \frac{m_e^2 U^3}{8\pi \ln \Lambda n e^4} \frac{m_p}{m_p + m_e}, \quad (43)$$

leads to the so called stopping length or penetration depth

$$\lambda_s = U t_s = \frac{m_e^2 U^4}{8\pi \ln(\Lambda) n e^4} \frac{m_p}{m_p + m_e} = \frac{1}{8\pi \ln(\Lambda) \rho e^4} E_e^2. \quad (44)$$

It is obvious that the stopping length and hence the column surface density $\rho \lambda_s$, where we used the fact $(m_p + m_e)n = \rho$, to slow down an incident particle only depends on the square of its energy. The question arising is whether the incident particle reaches the photosphere, where it will be released as BB radiation, or not. In the case of the neutron star the accretion flow is supersonic and therefore almost carried by ions. The opacity of neutron stars outer layers is due to electron scattering (Thompson scattering). The condition for penetration is that the penetration depth is larger than the photon's mean free path through the surface, therefore

$$\frac{m_p^2 U^4}{8\pi n e^4 \ln \Lambda} \frac{m_e}{m_p} > \frac{1}{n \sigma_T} = \frac{3m_e^2 c^4}{8\pi n e^4} = \lambda_{mfp}. \quad (45)$$

Hence reexpressing this condition for the incident velocity

$$U > 2.6(m_e/m_p)^{\frac{1}{4}} \sim 0.4c. \quad (46)$$

It was encountered that the proton is freely falling, means $U = \frac{2GM_*}{R_*}$, which gives an upper limit for the neutron stars radius R_* . Since the neutron star is compact object, defined by $R_* < 6R_{grav}$, penetration is generally possible. E.g. for one solar mass neutron star its radius must be smaller than $\sim 18km$ what is obviously the case for most of neutron stars.

Three self-consistent column models have been investigated:

- Subcritical-accretion without shocks
- Subcritical-accretion with collisionless-shocks
- Radiation-dominated with shocks

In the first two cases, radiation pressure can be neglected. This is a simplification, since radiation acts to hinder the accretion flow.

Subcritical-accretion without shocks

The column is overwhelmed by the infalling matter and therefore compressed by its ram pressure. As a consequence the matter is heated and loses (infall) energy via Coulomb collisions. Here electrons and protons have same velocities. These are in order of the free fall velocity $v_{ff} \simeq \frac{c}{2}$, so the heavier ions dominate the effects of compression and collisions. One may ask how strong the stopping power y_0 , a 'substituted' optical depth with $d\tau = \frac{\sigma_{scat}}{m_p} dy$, of the flow is i.e. when does the inflow stop? To calculate this, take first the total energy of a proton $E_p = \frac{1}{8}m_p c^2 + m_p c^2 \sim 1 \cdot 10^6 keV$, second the 'stopping' surface density is $4.6 \cdot 10^{-11} \frac{g}{cm^2} (keV)^{-2}$, obviously $\propto E_p$ as shown above, and finally the stopping density is in order of $50 \frac{g}{cm^2}$. For the strong magnetic field next to the poles ($\geq 10^{12} G$) one can impose that the Larmor radius r_L of a gyrating particle is smaller than its Debye length λ_D . This relation is reversed, if the field is weak since $r_L \propto B^{-1}$ and the Debye length is independent of B . Due to this fact, it is unphysical to consider the trajectory as straight line instead of spiraling drift during a scattering event. Using the Fokker-Planck equation describing the time evolution of the probability distribution due to drift and diffusion results in a reduced stopping power y_0 . Define a stopping region as

$$y(z) = \int_z^\infty \rho(z') dz' \leq y_0, \quad (47)$$

where $\rho(z')$ is the mass density at height z' . As already mentioned y_0 is $\propto E^{-2}$ and it is reasonable to assume that within the stopping region the behaviour of the heating rate Λ_{coul} (due to Coulomb collisions) is uniform and of course goes to zero outside,

$$\Lambda_{coul} \Big|_{y \leq y_0} = \frac{L_{acc} \rho}{A y_0} \text{ergs}^{-1} \text{cm}^{-3}, \quad (48)$$

where A represents the cross-sectional area of the accretion column (i.e. f_{disk} , but not restricted to the surface). For thermal stability and steadiness reasons the heating has to be compensated by an effective cooling which is provided by radiation processes of the heated electrons, namely thermal Bremsstrahlung and Compton cooling (see e.g. Hujeirat & Camenzind (2000)). The particle cross section related to these two processes have resonance at $\nu = \nu_{cyc} (= \frac{eB}{2\pi m_e c})$ in the excitation function showing a severe influence of the magnetic field. This fact also includes cyclotron radiation automatically.

Assuming local thermal equilibrium (LTE) and Thompson scattering due (i.e. $d\tau = \frac{\sigma_T}{m_p} dy$) to highly ionized column the diffusion-dominated radiation flux F reads

$$F = -\frac{c}{3} \frac{du}{d\tau} = -\frac{4\sigma}{3} \frac{d(T_\gamma^4)}{d\tau} = -\frac{4\sigma m_p}{3\sigma_T} \frac{d(T^4)}{d}. \quad (49)$$

On the other hand F is supported by heating (rate) of the matter below the point under consideration and is just given by

$$F(y) = \int_{y_0}^y \Lambda_{cool} dz = \frac{L_{acc}\rho}{Ay_0}(y - y_0). \quad (50)$$

If we collect both equations above together it is obvious that the radiation density u is quadratic in y and a boundary condition for $y=0$ is obtained, namely

$$\frac{L_{acc}}{A} = \frac{m_p c}{3\sigma_T} \frac{du}{dy} \Big|_{y=y_0}. \quad (51)$$

Hence the flux and the energy balance can be expressed in terms of the radiation temperature, the optical depth τ , the density ρ and the electron temperature T_e since it modifies the Compton cooling and since it increases outwards. Another condition can be imposed by the hydrostatic equilibrium supported by gas (outer layer) and ram pressure and gravity (weight of the column matter) for the pressure P in the stopping region

$$P = nK_B T_e = \left(\frac{GM}{R_*^2} + \frac{\rho_0 v^2}{y_0} \right) y. \quad (52)$$

Outside this region the ram pressure is modified so that

$$P = \frac{GM}{R_*^2} y + \rho_0 v^2, \quad (53)$$

where the first term represents the gravitational pressure and the second term the ram pressure. v here denotes the free-fall velocity and ρ_0 the density of the infalling matter. Simulations (Meszaros et al. 1983) have shown that for typical stopping power in order of $30 - 60 \frac{g}{cm^3}$ there is a thin plane parallel section of the polecap with vertical height $h \leq R_*$.

Subcritical-accretion with collisionless-shocks

The timescale on which shocks occur is too short for coupling particles thermally. That's why in collisionless plasmas electrons and protons are thermally decoupled in shock regimes, so their temperature jumps independently after passing shocks as indicated in Figure 7

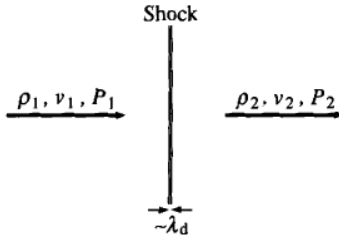


Figure 7: Shocks change plasma properties such as density or magnetic field

The temperature of ions and electrons, respectively, reads

$$T_i = \frac{3}{16} \frac{\mu m_H v_{ff}^2}{k} \quad (54)$$

and

$$T_e = \frac{5}{16} \frac{m_e v_{ff}^2}{k}, \quad (55)$$

where the statistical (thermal) equipartition theorem was used. The distinct prefactors are due to the degrees of freedom: electrons have two degrees less than ions. Ions are primarily heated by turbulent dissipation (Esin et al. 1996). Since $\mu m_H \sim 1800 m_e$ due to the great mass difference, electrons and ions temperature differ the factor $\sim 10^3 K$. As a consequence the ions will heat the electrons at a constant rate to bring them about equilibrium. The electrons in turn balance via cooling processes such as Bremsstrahlung and cyclotron emission. The dominating cyclotron radiation produces broadened spectral emission lines at each height h in the column around $\nu_{cyc} = \frac{eB}{\gamma m_e c}$ since the strength of B varies with position. An estimation of the shock height D can be done by using the timescale of equalizing temperatures, thus

$$D = \frac{v_{ff}}{4} t_{eq}. \quad (56)$$

Discussing accretion rates two cases arise: low and high accretion rates. Low \dot{M} imply a higher D which in return let vary the cyclotron frequency ν_{cyc} significantly. High \dot{M} imply a sufficiently small D which in turn let ν_{cyc} vary hardly (corresponds to a sharp line).

Radiation dominated column

The main idea of this model is based on the facts that there exist some luminous X-ray sources which cannot be described by the models above and the infalling gas is stopped by the radiation pressure i.e the photons which scatter rather on electrons than on protons which are decelerated due to the Coulomb force of the electrons. The magnetic pressure resists the radiation pressure $P_{rad} = \frac{1}{3} U_{rad}$ in transverse direction, the infall velocities of the matter however, are strongly hindered and confined by P_{mag} . A steady-state assumption simplifies the hydrodynamical equations, namely the continuity and the momentum equation (in z -direction) ,

$$\rho v = const. \quad (57)$$

$$\rho v \frac{\partial v}{\partial z} + \frac{1}{3} \frac{\partial U_{rad}}{\partial z} + \rho g = 0. \quad (58)$$

The gravity term $\rho g = \frac{GM\rho}{R_*^2} = \frac{\partial P}{\partial z}$ is negligible since its integrated form represents the weight of the gas in the column which pressure is small compared to the ram and radiation pressure. Hence integrating over z the both remaining terms result in

$$U_{rad} = 3\rho|v|(v_{ff} - v), \quad (59)$$

where $\rho v = const.$ and $U_{rad}(v_{ff}) = 0$ were used. The second means that sufficiently far above the stellar surface the infall is not hindered by radiation and

moves with free fall velocity. It already was used the assumption of a constant accretion rate $\dot{M} = -A\rho v$ which now becomes justified since ρv and column cross section A are constant. Note that the radiation pressure and infall velocity not only depend on the height z but also of transverse coordinates. This leads to the flux equation analogous to the first case plus a term representing the tendency of the inflow to scatter the photons downwards

$$\vec{F} = -\frac{cm_p}{3\sigma_T\rho}\vec{\nabla}U_{rad} + \vec{v}U_{rad}, = \frac{vm_p}{\sigma_T}\vec{\nabla}v + \vec{v}U_{rad} \quad (60)$$

where in the second step ∇U_{rad} was eliminated with the Eulerian equation. Here the first term stands for the net momentum flux of radiation before scattering and the second term after scattering. Taking the conversion of kinetic in radiative energy as instantaneous (no timescale), the divergence of the flux can be found as

$$\vec{\nabla}\vec{F} = -\rho v\vec{\nabla}\left(\frac{v^2}{2}\right). \quad (61)$$

Substituting with $Q = \left(\frac{v}{v_{ff}}\right)^2$ the radiation energy density reads

$$U_{rad} = 3|\rho v|v_{ff}(1 - \sqrt{Q}) = 3\rho v_{ff}^2(\sqrt{Q} - Q). \quad (62)$$

Inserting these two equations in the flux equation (the first term in the diffusion term of F , the second term in the 'downscatter' term) results in

$$\vec{F} = \frac{cm_p v_{ff}^2}{2\sigma_T}\vec{\nabla}Q + 3\rho v_{ff}\vec{v}(\sqrt{Q} - Q), \quad (63)$$

where in the first term was used that $|\rho v| = const$. Taking the divergence of this flux and equalizing with (61) gives

$$\nabla^2 Q = \frac{\sigma_T\rho|v|}{m_p c} \frac{\partial}{\partial z}(6\sqrt{Q} - 5Q). \quad (64)$$

Here, the Laplace operator is in cylinder coordinates. Together with boundary condition it is possible to determine the infall velocity $v(R, z)$ numerically. Then the density follows from the constant accretion rate, with which finally U_{rad} and \vec{F} are obtained. So it is necessary to give constraints on the boundary conditions:

- at stellar surface ($z = 0$): Q small, setting $Q = 0$
- at infinity ($z \rightarrow \infty$): $Q = 1$
- at cylindrical radius of column ($R = R_{col}$): $Q = 1$, since $U_{rad} = 0$

The latter is justified by the assumption that inside the column there is an optically thick regime in transverse (R) direction, and outside it is optically thin and therefore setting $U_{rad} = 0$. This is a very crude estimation, since this would imply a surface temperature of zero. So in the vicinity of the surface this

assumption is not applicable.

In the following picture a narrow region with dimensionless, cylindrical coordinates in r - and z -direction is shown. The contours a, b and c stand for different, constant velocities v_a, v_b and v_c , Q's respectively. These velocities decrease rapidly (from $v_a = 0.95v_{ff}$ to $v_c = 0.32v_{ff}$) in this narrow region; in turn, since ρv is constant the density ρ increase by the factor of ~ 3 as it is shown in Figure 8. This significant change of velocity and density in an exiguous regime is a clear indicator for a propagating shock wave. Thus the term 'radiative shock' for region between a and c is appropriate.

In this radiation-dominated shock scenario the effects of (strong) magnetic fields have been disregarded. Refined magnetic cross sections and more detailed treatment of radiation transfer could be reached by numerical simulations.

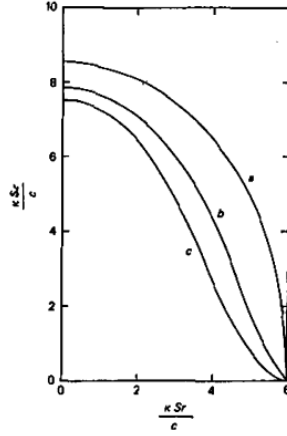


Figure 8: In a small plane in the column (expanded in r - and z -direction) the density and velocity change significantly

Still there is uncertainty of the continuity of the outflow (jet or blobs).

3.4 Accretion induced pulses in columns

The matter spiraling around the field lines towards the polecap produces synchrotron radiation. Detectable are pulses on a timescale of millisecond to hours. The nature of this phenomenon is explicable by the 'Leuchtturm' paradigm which consist of a NS with a rotation axis that has an angle the to the magnetic dipole axis and therefore the preceding magnetic field produces X-Ray synchrotron radiation by acting on the ionized gas of the accretion disk. The most significant property of pulsars is the rate of change of spin due to the exerting torques (Ghosh and Lamb, 1978).

4 Accretion powered Jets

4.1 Disk-Jet coupling

Observationally plasma jets are always connected with an accretion disk around a compact object. On the other side is any accretion disk responsible for a particle wind due to the release of gravitational energy. This gives rise to a strong connection of both occurrences. Efforts have been made by Blandford to draw models connecting disk, compact object and jet. The latter one not only removes matter else but also carry angular momentum from the disk. The role of a strong toroidal magnetic field (TMF) is important since it collimates the jet. The field lines have their feet in the disk corotate with the accretor since the field lines are 'frozen in'. When discussing jet collimation the effect called relativistic beaming has to be introduced. It is the process by which the relativistic effect modifies the apparent luminosity of the relativistic jet. It is of Particular importance for a jet which is oriented close to the line of sight. Jet kinematics can be simplified by considering them as a series of spherical clouds or blobs, each emitting a high luminosity. In the rest frame of the Earth each blob is approaching at speeds which can be in the range of $0.1 - 0.99c$, because of Special Relativity and some physical properties of the jet, the luminosity observed on Earth will be higher than the intrinsic luminosity measured in the rest frame of the jet clouds. The jet on the other side, however, moving away from Earth at relativistic speeds is affected quite differently. The observed luminosity from this counter-jet is less than the intrinsic luminosity (i.e luminosity in the jet frame) . locate

Plasma which transits from the disk to the jet drags magnetic field lines with itself. As a consequence the resulting field in the jet is twisted. Defining the hoop stress as stress/tension of circular configured magnetic field lines it is responsible for the collimation. There exist two explanative, idealized models for disk-jet connection: the Blandford-Payne and Blandford-Lovelace scenario. It is important to point out here for the case of neutron stars the connection cannot occur via the Blandford-Znajek process requiring a Black hole as the accretor. For AGN's having a black hole mass of $\sim 10^8 M_{\odot}$ the central engine which produces the enormous observed activity cannot be resolved geometrically by observations. Thus, a standard picture of an AGN has emerged to explain the richness of the radiation spectra:

- disk: emits mainly in the UV and soft X-rays on a scale of $2 - 100 R_{grav}$
- broad line 'clouds' (BLR): emits optically on scale of a few $1000 R_{grav}$ from center; can be scattered by hot e^-
- narrow line regions: emits mainly in the radio but also in the optical, UV and X-rays on a scale of $10^4 - 10^6 R_{grav}$

To illustrate such a coupling, a model for the disk-jet connection including a BH as accretor such as AGN's or Microquasars is presented in the next subsection.

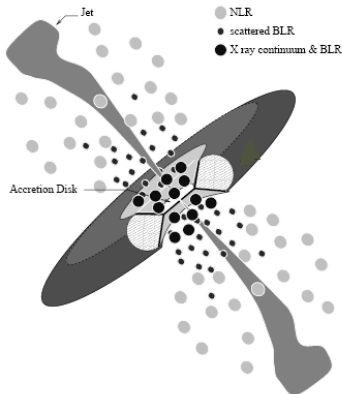


Figure 9: An overview of the different regions of the AGN disk-jet model each contributing to the resulting spectra. NLR and BLR stands for narrow line resonance and broad line resonance, respectively

4.2 A model of disk-jet connection for AGN's

The model presented in this section stems from Hujeirat (see Hujeirat 2004 and references there in). In this model a steady inflow-outflow configuration takes place. In the innermost part of the disk the strong magnetic field $B_p \propto R^{-2}$ suppresses the generation of turbulences. The matter inflow located nearby the equatorial plane of the disk (Regime 2) is threatened by a large scaled well-ordered PMF which is in super equipartition with the thermal energy inside a certain radius R_{tr} . In Regime 2 the rotation is sub-Keplerian. Outside R_{tr} (Regime 1) the PMF may be amplified by Balbus-Hawley and Parker instabilities giving rise to Dynamo generated turbulence and small-scaled, disordered magnetic fields. Next to 'inflow' regime in z-direction (θ -direction respectively) the highly dissipative transition layer (TL) is located (Regime 3). Here the matter moves outwards due to its super Keplerian rotation (Hujeirat & Camenzind (2002)). This inflow-outflow configuration let the 'frozen in' field lines exert a magnetic pressure. The angular velocity $\Omega(\theta)$ attains a maximum in θ -direction approximately at the height of the disk $H_d = r \sin(\theta)$ and therefore $\left. \frac{\partial \Omega}{\partial \theta} \right|_{H=H_d}$ changes sign. This yields two oppositely directed toroidal magnetic flux tubes (TMF). A part of the shear generated TMF reconnects while the other part is advected outwards collimating the jet (Hujeirat & Camenzind(2003)). Since there are two sides of an accretion disk (upper and under area) the accretion fulfils the following condition

$$\dot{M} \Big|_{tr} = 2\dot{M} \Big|_{BL}. \quad (65)$$

Via VLBI interferometry observations the total jet luminosity is detectable. In some AGN's such as the M87 jet the luminosity amounts to 10^{44} erg/s . Constraints on the input parameters in the problem such as geometry and magnetic field can be numerically found by using 3D axis-symmetric radiative MHD equations (see e.g. Hujeirat, Camenzind & Keil (2008))

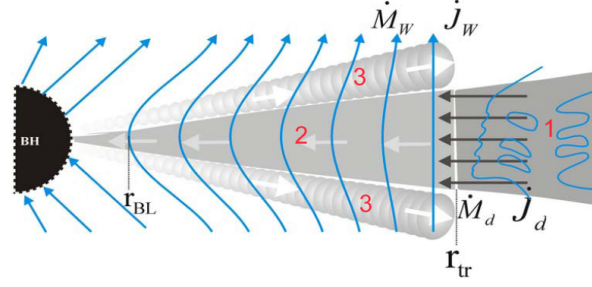


Figure 10: steady infow-outflow configuration and magnetic field lines in the three regimes described above

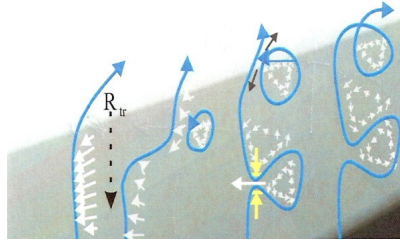


Figure 11: The transition of regime 1, where fields are on microscopic scales, to regime 2, where the magnetic field becomes large-scale ordered

4.3 Jet

A polar jet is a phenomenon, where streams of matter are emitted along the axis of rotation of a compact object. It is caused by the dynamic interactions within an accretion disc of cataclysmic variables and X-ray binaries. When matter is emitted at velocity $v \sim c$ these jets are called relativistic jets. Relativistic jets are extremely powerful outward-orientated motion of plasma which emerge from the centers of some AGN's and quasars. In the case of neutron stars the jet can be ultra-relativistic in some cases (Fender et al. 2004) and have mostly relativistic outflows. The length scale of the jet can reach several parsecs (Heinz et al. 2007). Therefore neutron stars are as important as black holes in producing jets. Because relativistic jets are believed to be launched in the inner regions of accretion disks, that is from the boundary layer, they are important probes of strong gravity and the physics of compact objects. Still open is the question of the matter content of the jet. Is it rather leptonic pair plasma ($e^+ - e^-$ dominated) or baryonic plasma ($p - e^-$ dominated)? Although Reynolds (Reynolds et al. 1996) proposed that the jet in M87 is most likely pair dominated, one may not conclude that in quasars jets are also $e^+ - e^-$ dominated. not an exclusion of a possible baryonic plasma. Another investigation is to check whether the jet is an *hydromagnetic outflow*, which have a significant mass flux and which have the energy and angular momentum carried by both the matter and the electromagnetic field, or *Poynting flux*, in which the mass flux is negligible and the energy and angular momentum are carried predominantly by the electromagnetic field. Both outflows exist: a quasi-stationary collimated Poynting jet arises from the

inner part of the disk while a steady uncollimated hydromagnetic outflow arises in the outer part of the disk (Lovelace & Romanova (2009)).

5 Conclusion

Jets have been observed in X-ray binaries, in active galactic nuclei and in quasars. Recent observations have revealed that jets with high Lorentz factors do not only emanate from micro-quasar systems, but from systems containing neutron stars (Fender et. al (2004)). Taking into account the correlation between the maximum propagational speed of jet-plasmas with the maximum penetration of the accreted matter in the gravitational well of the central accreting NSs, we conclude that these NSs are residing inside their last stable orbits, hence the origin of their ultra-compactness. So accretion disk surrounding neutron stars have many similarities to AGN's: in both cases the inflow next to the surface is magnetically controlled. Due to the redistribution of angular momentum extraction of rotational energy on electromagnetic ways occurs. In the case of neutron stars there are accretion columns, which transports matter from the disk to the polecaps. No collisions happen in these columns, but shocks can occur as in the radiation dominated column but also in the gas pressure dominated one.

There is a clear link between accretion disk and jet. This conversion from accretion inflow to jet outflow needs a gravitational strong engine with a geometrically small expansion, namely compact objects. This can be quasars of a few solar masses, but also AGNs of billion solar masses. Accretion-jet spectra consist of several components and have some common characteristics such as the X-ray continuum. Jets are often collimated and reaches several parsecs. Their geometry is given by narrow spiraled magnetic field lines along axis of rotation. The matter content of collimated jets seems to be rather leptonic, i.e. a e^-e^+ -pair plasma, than hadronic, i.e. e^-p - plasma, although a hadronic outflow cannot be disregarded since there are still geometric uncertainties (Reynolds et al. 2006).

In the forthcoming time, I intend to modify this preliminary work into a Master thesis, in which, by means of general relativistic magneto-hydrodynamical calculations, the formation of shocks in the polar cap will be simulated. The calculations would be carried using the solver GR-I-RMHD developed by the computational group of Hujeirat and Camenzind.

References

- [Basko & Sunyaev (1976)] Basko, M.M., Sunyaev, R.A., 1976, 'The limiting luminosity of accreting neutron stars with magnetic fields', *MnRAS* 175, 395
- [Biretta et al.(1995)] Biretta, J.A., Zhou, F., Owen, F.N., 1995, 'Detection of proper motions in the M87 jet', *ApJ*, 447, 582-596
- [Boyd & Sanderson (1969)] Boyd, T.J.M., Sanderson, J.J., 1969, 'Plasma dynamics', ch.10, Thomas Nelson & Sons
- [Burgarella & Livio (1993)] Burgarella, D., Livio, M., O'Dea, C.P., 1993, 'Astrophysical jets', Cambridge University press
- [Esin et al. (1996)] Esin, A.A., Narayan, R., Ostriker, E., Yi, I., 1996, 'Hot one-temperature accretion flows around black holes', *ApJ* 465, 312-326
- [Fender et al. (2004)] Fender, R., Wu, K., Johnston, H., Jonker, P., Spencer, R., van der Klis, M., 2004, 'An ultra-relativistic outflow from a neutron star accreting gas from a companion', arXiv:astro-ph/9812150v1
- [Frank et al.(1992)] Frank, J., Raine, A., Raine, D., 1992, 'Accretion power in astrophysics (Third edition)', Cambridge University press
- [Gosh & Lamb (1978)] Ghosh, P., Lamb, F.K., 1978, 'Disk accretion by magnetic neutron stars', *ApJ* 223, L83-87
- [Hawley et. al (1998)] Hawley, J.F., Balbus, S.A., Winters, W.F., 1998, 'Local Hydrodynamic Stability of Accretion Disks', arXiv:astro-ph/9811057
- [Heinz et al. (2007)] Heinz, S., Schulz, N.S., Brandt, W.N., Galloway, D.K., 2007, 'Evidence of a parsec-scale X-ray jet from the accreting neutron star Circinus X-1', *ApJ* 663, L93-L96
- [Hujeirat (2004)] Hujeirat, A., 2004, 'A model for electromagnetic extraction of rotational energy and formation of accretion-powered jets in radio galaxies' *Astronomy and Astrophysics*, 416, 423435
- [Hujeirat & Camenzind (2000)] Hujeirat, A., Camenzind, M., 2000, 'Truncated disks - advective tori solutions around BHs. I. The effects of conduction and enhanced Coulomb coupling', *Astro. and Astrophysics*, 362, 41
- [Hujeirat & Camenzind (2002)] Hujeirat, A., Camenzind, M., Livio, M., 2002, 'Ion-dominated plasma and the origin of jets in quasars', *Astro. and Astrophysics*, 394, 9
- [Hujeirat & Camenzind (2003)] Hujeirat, A., Livio, M., Camenzind, M., Burkert, A., 2003, 'A model for the jet-disk connection in BH accreting systems', *Astro. and Astrophysics*, 408, 415

- [Hujeirat, Camenzind & Keil (2008)] Hujeirat, A., Camenzind, M., Keil, B.W., 2008, 'An implicit numerical algorithm for solving the general relativistic hydrodynamical equations around accreting compact objects', *New Astronomy Journal*, 13, 436
- [Hujeirat & Thielemann (2009)] Hujeirat, A., Thielemann, F.-K., 2009, 'Angular momentum transport during X-ray bursts in neutron stars: a numerical general relativistic hydrodynamical study', *Astro. and Astrophysics*, 496, 609
- [Issi Bern] issibern.ch
- [Lamb (1977)] Lamb, F.K., 1977, 'Knowledge of neutron stars from X-ray observations', *Annual New York Academy of Sciences*, 302, 482-513
- [Laming (2009)] Laming, J.M., 2009, 'Collisionless shock wave', *Scholarpedia*, 4(7), 6071
- [Liou et. al.(1993)] Liou, X., Yang, P., Yang, L., Chen, S., 1993, 'The radial structure of hot one-temperature accretion flows with advection', *ChinAstroph* Vol.21/4, 404-414
- [Lovelace & Romanova (2009)] Lovelace, R.V.E, Romanova, M.M., 2009, 'Launching of Poynting jets from accretion discs', *astro-ph.HE*, 29 Jan 2009
- [Meszaros & Ostriker (1983)] Meszaros, P., Ostriker, J.P., 1983, 'Shocks in Spherically Accreting Black Holes: A Model for Classical Quasars', *ApJ* 273, L59-65
- [Müller] Müller, A., 2009, 'www.wissenschaft-online.de'
- [Oort (1981)] Oort, J.H., 1981, 'Annual Review of Astronomy and Astrophysics', Vol. 19, sections 1-4
- [Rees et al. (1982)] Rees, M.J., Begelman, M.C., Blandford, R.D., Phinney, E.S., 1982, 'Ion-supported tori and the origin of radio jets, *Nature* Vol. 295
- [Reynolds et al. 1996] Reynolds, C.S., Fabian, A.C., Celotti, A., Rees, M.J., 1996, 'The matter content of the jet in M87: evidence for an electron-positron jet', *MnRAS* 283, 873-880
- [Rybicki (1979)] Rybicki, G.B., Lightman, A.P., 1979, 'Radiative processes in astrophysics', Wiley-VCH Verlag
- [Sauty (2001)] Sauty, C., Tsinganos, K., Trussconi, E., 2001, 'Jet Formation and Collimation in AGN and μ -Quasars', [arXiv:astro-ph/0108509v1](https://arxiv.org/abs/astro-ph/0108509v1)
- [Spacetime travel] www.spacetimetravel.org
- [Ustyugova et. al.(2000)] Ustyugova, G.V., Lovelace, R.V.E., Romanova, M.M., Li, H., Colgate, S.A., 2000, 'Poynting jets from accretion disks: Magneto-hydrodynamic simulations', *ApJ* 541: L23-26

[Venables] Venabeles, J., venables.asu.edu

[Vietri (2008)] Vietri, M., 'Foundations of high-energy astrophysics', the University of Chicago press

[Wikipedia] wikipedia.en.